IEEE Access
Multidisciplinary | Rapid Review | Open Access Journal

Received November 10, 2020, accepted November 26, 2020, date of publication December 11, 2020,
date of current version December 28, 2020.

Digital Object Identifier 10.1109/ACCESS.2020.3044194

Galerkin Finite Element Based Modeling of One Dimensional Packed Bed Reactor for Underground Coal Gasification (UCG) Process

QUDSIYA IRUM[1], SHAHID A. KHAN[1], ALI ARSHAD UPPAL[1], (Member, IEEE), AND LILIA KRIVODONOVA[2]

[1]Department of Electrical and Computer Engineering, COMSATS University Islamabad, Islamabad 45550, Pakistan
[2]Department of Applied Mathematics, University of Waterloo, Waterloo, ON N2L 3G1, Canada

Corresponding author: Qudsiya Irum (qudsiya.irum@comsats.edu.pk)

ABSTRACT Mathematical models of a complex physicochemical underground coal gasification process involve multidimensional non-linear partial differential equations (PDEs). Therefore, researchers always seek a suitable numerical scheme that would give a good balance between accuracy of the solution and computational complexity. In this paper, the non-linear PDEs describing energy and mass balances of both coal and char are solved by Galerkin finite element method (GFEM). The infinite-dimensional spatial domain is transformed into a finite number of elements, whose dynamics are governed by a system of ordinary differential equations (ODEs). Owing to the execution of GFEM, the time domain and space-dependent first-order ODEs for solids (coal and char) and gases are solved numerically to find a solution of the UCG process. The resultant syngas compositions and the calibrated heating value are influenced by the operation parameters and the type of oxidant used. The results are compared with the experimental data obtained from the Thar coal UCG site, and with existing work, based on the finite difference method (FDM) for the one dimensional (1D) model. The simulated results along with the quantitative analysis show the superiority of the GFEM model over the FDM model.

INDEX TERMS Energy conversion process, Galerkin finite element method, packed bed reactor, process modeling, underground coal gasification (UCG).

I. INTRODUCTION

The underground coal gasification (UCG) is a clean coal conversion technology in which in-situ coal deposits are gasified into useful gas products called syngas, which is mainly a mixture of H_2, CO_2, CO, and CH_4 [1]. The process starts by drilling a pair of vertical wells (injection and production) into the coal seam. High pressure air is used to increase the natural permeability of coal that forms a pneumatic link. The wells are at a prescribed distance from each other, and are linked by a process of Reverse Combustion Linking to allow the transfer of gases through them [2]. Then, air or a gas mixture of O_2 and steam is injected as an oxidizing agent via injection well. The syngas is recovered from the production well and can be later used for a number of industrial applications [3], [4]. Pakistan is considered a coal-rich country after the discovery of lignite-B type coalfield reserves (175.5 billion tonnes) in Tharparker district of Sindh province which covers an area of over 9,100 sq.km [5]–[7]. Due to the on-site geological conditions and type of the coal, UCG is the most suitable and environment friendly technology to harness these coal reserves and to overcome the shortfall of energy in Pakistan [8], [9].

Computational modeling and simulation tools are important to address the feasibility studies and quantitative understanding of a complex process like UCG before a field scale test. There are several field and laboratory-scale UCG reactor models which are being tested and operated all over the world. The most popular model is a packed bed reactor model that describes the overall field performance of UCG [10]. The packed bed model simulates gasification with a stationary coal bed in a highly permeable porous media and is consumed over the time [11]. According to Gunn and Whitman [12], the lignite and sub-bituminous based coal

The associate editor coordinating the review of this manuscript and approving it for publication was Paolo Bettini.

seam gasification resembles the operation of a packed bed chemical reactor so they developed a linear mathematical model for forward combustion of UCG. They transformed the PDEs for mass balances and individual gas species into ODEs using the finite difference method (FDM) and predicted the exhaust dry gas composition, gas heating value, thermal energy, and efficiency during the gasification process. Thorsness and Rozsa [13] provided the calculational modeling of permeable packed bed reactor and validated the results with lab-scale experiment. Thorsness *et al.* [14] developed a 1D model of sub-bituminous coal based packed bed reactor using FDM discretization of mass and energy balances of the solids. They conducted a lab-scale experiment to observe the product gas composition and thermal front propagation. Winslow [15] followed the physical and chemical model of Thorsness *et al.* [14] but he did not approximate any stationary phase for conservation equations and an implicit method was used to solve non-linear PDEs. Abdel-Hadi and Hsu [16] developed a pseudo-2D model on a rectangular domain by using the governing equations of Winslow [15] and transformed the equations to a new coordinate system. A progressive configuration of gasification zone at several stages was also calculated. Khadse *et al.* [17] developed a 1D model by taking the chemical and pseudo-steady state fluid flow model of Thorsness *et al.* [14] to analyze the solid compositions in the UCG process and the effects of model parameters on temperature. But, the authors slightly changed the input values of initial porosity, initial feed temperature, concentration of O_2, N_2, and steam/O_2 ratio. Their results were only in a qualitative agreement with the experimental results of Thorsness *et al.* [14]. Uppal *et al.* [18] developed a packed bed mathematical model using FDM technique for solid phase mass and energy balances and optimized the input parameters. They utilized the experimental inlet gas flow rate from the UCG project of Thar coal field and calculated the composition and heating value of the product gas to validate with experimental data. The model also employed a sliding mode control scheme to maintain a desired heating value [19].

A comprehensive UCG model incorporates a complex range of physical phenomena like mass transfer, heat transfer, coal pyrolysis, and complex chemical reactions for investigation of the reactive behavior of coal gasification. In numerical modeling of UCG, the FD (finite difference) discretization scheme has been used in literature in numerical solution of the continuum problem but it can give value at particular points only and cannot be used to evaluate the values at the desired points between two grid points. Also, it is computationally expensive, especially if higher accuracy is required. For these limitations of the FDM, we used GFEM technique to find numerical solutions of nonlinear boundary value problems. Because GFEM gives a polynomial at each point within the domain and one can easily use the finite element shape functions instead of trial functions [20]–[26]. The GFEM uses an integral form of the PDEs to yield a semi-discretized system of ODEs satisfying the boundary conditions [27]–[30]. The time coordinate also needs to be discretized into a sequence of time intervals, require an iteration method because the time dependent variable affects the future solution only [31]. The discretization and adjoints commute in GFEM which also helps in optimization of parameters [32].

In this work, the gasification channel in the UCG process is assumed to be a packed bed reactor. The mass and energy balances of coal and char are viewed as PDEs while the mass and energy balances of gas phase as ordinary differential equations (ODEs). The GFEM based simplified finite-dimensional computational models of coal and char densities and the coal temperature developed for the UCG process model are described in [18], [33]. The results of modeling predict coal consumption, changes of temperature, gas composition, and the heating value. The chemical and physical properties of lignite-B coal and the operating conditions of Thar UCG project in Pakistan are used in the simulations. We have compared the computational results obtained by GFEM with the FDM based packed bed model (given in [34]). We have also validated our computations using the experimental data. The results are depicted graphically as well as in tabular form.

The paper is composed as follows. The mathematical model of UCG reactor which describes the mass balance, energy balance, Darcy's law, and gas velocity is presented in Sect. II. The GFEM models of solid phase PDEs for both solid coal and char are described in detail in Sect. III. The solution strategy followed during computation is explained in Sect. IV. The obtained numerical results are discussed in Sect. V. The GFEM model validation is performed against the FDM model with respect to experimental data in Sect. VI. Finally, the paper is concluded in Sect. VII.

II. UCG REACTOR MODEL

The UCG reactor model of Uppal *et al.* [18] is adapted in this work, as shown in Fig. 1. This model is comprised of eight gases: CO, CO_2, H_2, $H_2O_{(g)}$, CH_4, N_2, O_2, and tar, and

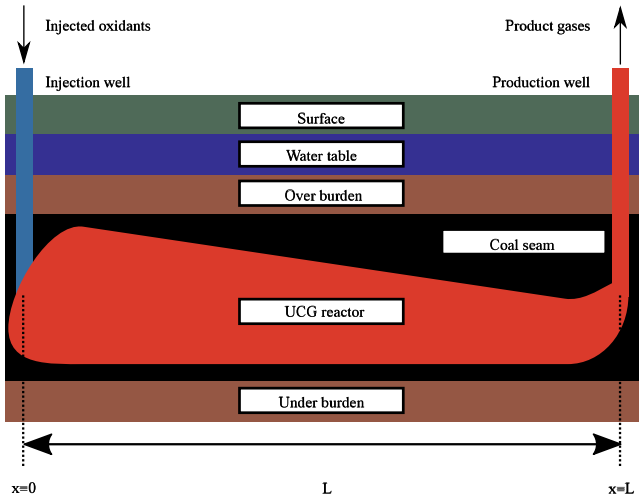

FIGURE 1. Schematic of UCG process [18].

two solids: coal and char. The mathematical equations are obtained from mass and energy balances of solids and gases.

A. MASS BALANCE OF COAL AND CHAR

Equation (1) describes the mass balance of coal as a solid specie that is consumed within the UCG reactor by pyrolysis reaction over time.

$$\frac{\partial \rho_1}{\partial t} = M_1\, r_1,$$
$$\text{I.C}: \ \rho_1(0, x) = \rho_{1_0}(x), \ 0 \le x \le L. \tag{1}$$

Equation (2) is the mass balance equation for char produced during pyrolysis reaction and then consumed by oxidation and gasification reactions.

$$\frac{\partial \rho_2}{\partial t} = M_2 \sum_{j=1}^{6} a_{s_j} r_j,$$
$$\text{I.C}: \ \rho_2(0, x) = \rho_{2_0}(x), \ 0 \le x \le L. \tag{2}$$

B. ENERGY BALANCE OF COAL

Equation (3) is the energy balance of the solids, which depicts the effect of convective and conductive heat transfer on solid temperature. Moreover, the change in temperature due to the chemical reactions is characterized by the source term H_s. The initial condition shows that the temperature is known at a time t_0. The values of spatial derivatives at $x = 0$ and $x = L$ constitute the Neumann type boundary conditions. The homogeneous boundary conditions mean that the ends of the reactor are insulated and no heat flux can enter or leave the reactor [33].

$$C_s \frac{\partial T_s}{\partial t} - \frac{\partial}{\partial x}\left[(1-\phi)k \frac{\partial T_s}{\partial x}\right] - h_t(T - T_s) = -H_s.$$
$$\text{I.C}: T_s(0, x) = T_{s_0}(x), \ 0 \le x \le L,$$
$$\text{B.C}: \frac{\partial T_s}{\partial x}(t, 0) = \frac{\partial T_s}{\partial x}(t, L) = 0, \ t \ge 0.$$
$$C_s = \sum_{i=1}^{2} \rho_i c_{s_i}, \ H_s = \sum_{j=1}^{5} \Delta H_j r_j. \tag{3}$$

The physical parameters in (1), (2), and (3) are described in Table 1. The description of h_t, k, and the chemical reaction rates is given in Appendix A and B respectively.

C. MASS BALANCE OF GAS

Equation (4) describes the change in concentration of the gas due to various chemical reactions, when it moves from the inlet to the outlet well.

$$\frac{dC_i}{dx} = \frac{1}{u_g}\left(-C_i \frac{du_g}{dx} + \sum_{j=1}^{6} a_{ij} r_j\right). \tag{4}$$

D. ENERGY BALANCE OF GAS

The temperature of gas in (5) tends to vary due to convective heat transfer effects from the injection to production well.

$$\frac{dT}{dx} = -\frac{1}{u_g C_g}\left[h_t\,(T - T_s) + H_g\right],$$

TABLE 1. Physical parameters used in the model.

Symbol	Description	Unit
ρ_1, ρ_2	density of coal and char respectively	g/cm^3
M_1, M_2	molecular weight for coal and char, respectively	g/mol
r_j	rate of j^{th} chemical reaction, j=1,..,6 represents pyrolysis, char oxidation, steam gasification, CO_2 gasification, methanation and water gas shift reaction respectively	$mol/cm^3/s$
a_{s_j}	stoichiometric coefficient of solid in j^{th} reaction	
C_s	total heat capacity of solids	$cal/K/cm^3$
c_{s_i}	specific heat capacity of component	$cal/g/K$
k	effective thermal conductivity	$cal/cm/s/K$
h_t	heat transfer coefficient	$cal/s/K/cm^3$
H_s	solid phase heat source	cal/mol
T_s, T	solid and gas temperatures respectively	K
ϕ	coal bed porosity	
L	Reactor length	cm

$$C_g = \sum_{i=1}^{6} C_i c_{p_i}, \ H_g = \Delta H_6 r_6. \tag{5}$$

E. DARCY's LAW

The drop of pressure for the gas mixture is modeled by (6).

$$\frac{dP}{dx} = -\frac{u_g \mu}{2K}. \tag{6}$$

F. GAS VELOCITY

Equation (7) represents the gas phase hypothetical velocity in the porous media of UCG reactor.

$$\frac{du_g}{dx} = -\frac{u_g}{P}\frac{dP}{dx} + \frac{u_g}{T}\frac{dT}{dx} + \frac{RT}{P}\sum_{i=1}^{8}\sum_{j=1}^{6} a_{ij} r_j. \tag{7}$$

The gas phase equations are only ODEs in length domain due to quasi steady state approximation because all the conductive transport is lumped in solid phase and accumulation terms are neglected in the gas equations. The gas velocity ranges from 36-360 m/hr, while the rate of coal burning is only 0.1-0.2 m/hr. Therefore, it can be assumed that the gas phase reaches steady state before any significant change occurs in solids [13], [17], [18], [33], [34].

The parameters of the gas phase (4), (5), (6), (7) are described in Table 2.

In the following section, application of GFEM on solid phase PDEs is discussed in detail.

III. GFEM MODEL OF UCG PROCESS

A. GFEM MODEL FOR HEAT EQUATION

First, we consider (3) for prediction of the temperature distribution of solid coal in reactor bed. The GFEM model of the heat equation requires discretization of the spatial domain into finite elements. Thus, multiplying (3) by a test function N_i, integrating the result over the computational domain [0, L] [35] while evaluating the thermal conductivity term by the product rule and stiffness term by the integration by parts

TABLE 2. Gas phase parameters and states.

Symbol	Description	Unit
C_i	concentration of gas i, i = 1, ..., 8	mol/cm^3
u_g	flow rate of air	$mol/cm^2/s$
C_g	total heat capacity of gas	cal/mol/K
c_{p_i}	molar heat capacity of gas i	cal/mol/K
ΔH_j	heat of reaction	cal/mol
H_g	gas phase heat source	cal/mol
a_{ij}	stoichiometric coefficient of gas i in j^{th} chemical reaction	cal/g/K
P	gas pressure	atm
v_g	gas velocity	cm/s
K	permeability coefficient	
R	universal gas constant	$cm^3 \cdot atm/mol/K$
μ	viscosity	cP

rule results in:

$$C_s \int_0^L \frac{\partial T_s}{\partial t} N_i(x)dx + (1-\phi)2k \int_0^L \frac{\partial T_s}{\partial x}\frac{\partial N_i(x)}{\partial x}dx - \int_0^L h_t (T - T_s) N_i(x)dx = -\int_0^L H_s N_i(x)dx. \quad (8)$$

Since,

$$\int_0^L \frac{\partial}{\partial x}\left(k\frac{\partial T_s}{\partial x}\right) N_i(x)dx = k\left(N_i(x)\frac{\partial T_s}{\partial x}|_0^{LL} - \int_0^L \frac{\partial T_s}{\partial x}\frac{\partial N_i(x)}{\partial x}dx\right) + k\int_0^L \frac{\partial^2 T_s}{\partial x^2} N_i(x)dx$$

Here, $N_i(x)$ is a test function, $1 \leq i \leq N$, N is total number of nodes.

In the Galerkin method, the same set of functions is utilized for the basis and test functions. Introducing a mesh, $0 \leq x \leq L$ with element size $h_j = x_j - x_{j-1}$, we choose an approximation in a finite-dimensional subspace.

$$T_s(x, t) = \sum_{j=1}^{N} T_{s,j}(t) N_j(x), \quad (9)$$

where the solid temperature $T_{s,j}$, $j = 1, 2 \ldots N$, is a function of time t and $N_j(x)$ is a piece-wise linear polynomial defined as:

$$N_j(x) = \begin{cases} \frac{x - x_{j-1}}{x_j - x_{j-1}}, & x_{j-1} \leq x \leq x_j \\ \frac{x_{j+1} - x}{x_{j+1} - x_j}, & x_j \leq x \leq x_{j+1} \\ 0, & \text{elsewhere.} \end{cases}$$

With a uniform element size h, (8) becomes:

$$C_s \sum_{j=1}^{N}\left[\int_0^L \frac{dT_{s,j}}{dt} N_i N_j dx\right] + 2(1-\phi)k \sum_{j=1}^{N}\left[\int_0^L T_{s,j}\frac{dN_i}{dx}\frac{dN_j}{dx}dx\right] + h_t \sum_{j=1}^{N}\left[\int_0^L T_{s,j} N_i N_j dx\right] - h_t \int_0^L T N_i dx = -\int_0^L H_s N_i dx. \quad (10)$$

Let A_i and M_i, $i = 1, 2, .., N$, be the local stiffness and mass matrices, respectively.

$$A_i = \sum_{j=1}^{N}\left(\int_0^L \frac{dN_i}{dx}\frac{dN_j}{dx}dx\right),$$

$$M_i = \sum_{j=1}^{N}\left(\int_0^L N_i N_j dx\right).$$

We combine contributions from the element matrices (A_i and M_i) into the global stiffness matrix **A** and global mass matrix **M** by expanding each element matrix and vector to dimension N.

$$A = \frac{1}{h}\begin{bmatrix} 2 & -1 & 0 & 0 & \cdots & 0 \\ -1 & 2 & -1 & 0 & \cdots & 0 \\ 0 & -1 & 2 & -1 & \cdots & 0 \\ \cdots & \cdots & \cdots & \cdots & \cdots & \cdots \\ 0 & 0 & \cdots & 0 & -1 & 2 \end{bmatrix},$$

$$M = \frac{h}{6}\begin{bmatrix} 4 & 1 & 0 & 0 & \cdots & 0 \\ 1 & 4 & 1 & 0 & \cdots & 0 \\ 0 & 1 & 4 & 1 & \cdots & 0 \\ \cdots & \cdots & \cdots & \cdots & \cdots & \cdots \\ 0 & 0 & \cdots & 0 & 1 & 4 \end{bmatrix}.$$

For the entire spatial domain, the finite element discretization results in a system of ODEs with continuous representation of time. A fully discretized model requires a further approximation of ODEs to obtain a set of algebraic equations.

Equation (10) can be written in the matrix form as:

$$M\frac{dT_s}{dt} = \frac{hh_t T - H_s - 2k(1-\phi)AT_s(t) - h_t M T_s(t)}{C_s}. \quad (11)$$

In a time dependent problem, a disturbance can only influence a part of domain. The Forward Euler method carries information forward in time [36]. To get updated time profiles of the solid temperature in (11),

$$MT_{s,k+1} = \left(\frac{hh_t T - H_s - 2k(1-\phi)AT_{s,k} - h_t M T_{s,k}}{C_s}\right)dt + MT_{s,k}. \quad (12)$$

This formulation implies that once the solution of solid temperature at k, $1 \leq k \leq n$, discretization points in time, is known at a given time t then (12) explicitly gives the solution at time $t+\Delta t$.

B. GFEM MODEL FOR COAL DENSITY

The PDE describing the mass balance of coal in (1) is also discretized to obtain the GFEM formulation.

$$\int_0^L \frac{\partial \rho_1}{\partial t} N_i(x)dx = M_1 \int_0^L r_1 N_i(x)dx. \tag{13}$$

The approximation of coal density in terms of a piece-wise linear basis function is:

$$\sum_{j=1}^{N} \left[\int_0^L \frac{\rho_{1_j}}{dt} N_i N_j dx \right] = M_1 \sum_{j=1}^{N} \left[\int_0^L r_1 N_i N_j dx \right]. \tag{14}$$

Equation (14) can be written in the matrix form as:

$$M\frac{d\rho_1}{dt} = 5M\rho_1 \exp\left(-\frac{6039}{T_s}\right). \tag{15}$$

The time discretization of (15) by the Forward Euler method yields the updated value of coal density.

$$\rho_{1,k+1} = 5\rho_{1,k}\exp\left(-\frac{6039}{T_s}\right) dt + \rho_{1,k}. \tag{16}$$

C. GFEM MODEL FOR CHAR DENSITY

Now, the GFEM model of the char density from (2) is developed as follows,

$$\int_0^L \frac{\partial \rho_2}{\partial t} N_i(x)dx = M_2 \int_0^L \left(\sum_{j=1}^{6} a_{s_j} r_j \right) N_i(x)dx. \tag{17}$$

Multiplying (17) by a test function N_i, $i = 1, \ldots, N$, while taking approximate solution of char density in terms of a piece-wise linear polynomial function N_j, $j = 1, \ldots, N$ and integrating over the computational domain [0, L], we obtain a matrix form.

$$M\frac{d\rho_2}{dt} = hM_2 \sum_{j=1}^{6} a_{s_j} r_j. \tag{18}$$

We solve (18) using the Forward Euler method.

$$M\rho_{2,k+1} = hM_2 \sum_{j=1}^{6} a_{s_j} r_j + M\rho_{2,k}. \tag{19}$$

IV. SOLUTION STRATEGY

The solution procedure is described in the flow chart in Fig. 2. The model comprises the set of PDEs for solid phase balance equations and ODEs for gas phase balance equations. The input parameters for coal are density and temperature and for gas are concentration, temperature, and pressure. We begin by initializing the solid and the gas phase systems at $t = 0$ second. For solution of the system of ODEs, an implicit TR-BDF2 method is used, which is a one-step numerical scheme

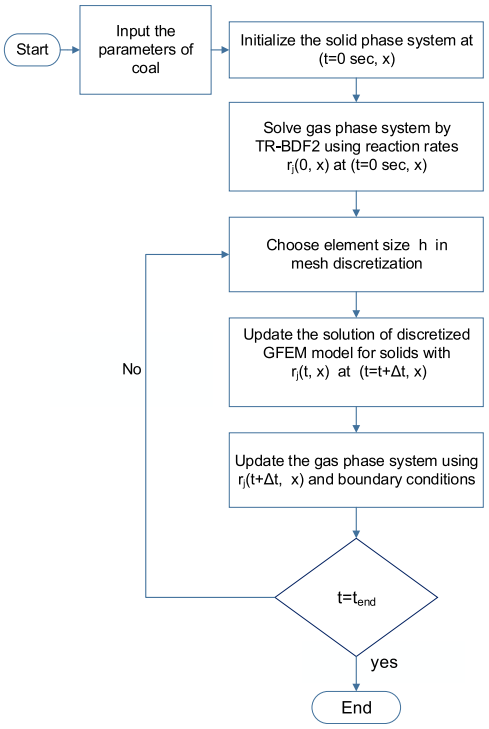

FIGURE 2. Solution strategy for GFEM based UCG packed bed reactor model.

for stiff problems [37], [38]. The overall solution of the system advances in time due to the solid equations, whereas, the gas phase system inculcates the dynamics against the length of the reactor. After the initialization, the set of discretized solid phase algebraic equations given in (11), (15), and (18) are computed at the new time level to get updated profiles of solid-temperature, solid-densities, and reaction rates. Then, the gas phase species (4), (5), (6), and (7) are updated at the new time level to generate new estimates of the gas temperature and concentrations. Selection of element size h in GFEM model is important in space discretization [36], [39]. Therefore, different element sizes have been tested and it was found that the numerical solution approaches the field outcomes if a mesh with $h <= 0.5$ cm is used. The procedure is repeated until the final time t_{end}.

The input parameters used in MATLAB simulations are specified in Table 3.

V. NUMERICAL RESULTS AND DISCUSSION

The computed solutions of GFEM based numerical model for the UCG reactor demonstrate various features of the simulation. The volatile matter in coal is released first in the reactor at low heating rates. Then char reacts with an oxidizing agent at higher temperatures to yield the gaseous products. We show in Fig. 3 the behavior of temperature distribution along the length of the coal bed reactor at different times. The movement of the gasification process associates the reaction and pyrolysis fronts at different speeds. The coal pyrolysis front is followed by the char reaction front, as shown in Fig. 3.

TABLE 3. Input parameters for simulation.

Input Parameter	Value
coal type	Lignite-B, Thar coal
reactor length	2500 cm
inlet gas temperature	430 K
inlet gas pressure	6180.8 k dynes/cm^2
input particle diameter	1 cm
initial coal density	1.113 (g/cm^3)
coal porosity	0.2
molecular weight of coal	20 g/mol
coal permeability	150
oxygen concentration	21%
time step size Δt	2 s
element size h	0.4 cm (for discretized solids only)

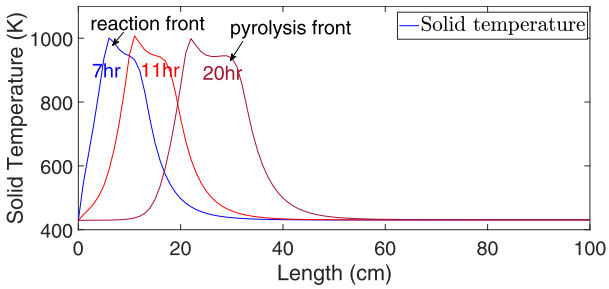

FIGURE 3. Solid temperature at three different times for 1 m reactor simulation.

At the reaction front, the exothermic chemical reactions occur and the gases flow in opposite direction. The close-up of temperature profiles show that the reaction zone expands with time.

The gas temperature profile shown in Fig. 4 only accounts for heat transfer through convection. Finally, the solid and gas temperatures reach the thermal equilibrium value.

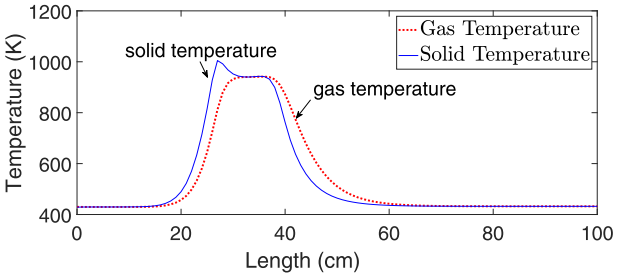

FIGURE 4. Calculated solid and gas temperatures after at t=20 hrs.

Profile of the coal and char densities in Fig. 5 and Fig. 6 demonstrate that wet coal has dried and char has been produced at the pyrolysis front, which is then consumed at the reaction front. It can be seen that the width of spatial profiles of solid temperature (Fig. 3) and char density (Fig. 6) increases as the process advances in time. This necessarily indicates that the reaction zone is widening with time.

Average reaction rates that occurred over the length of the reaction zone at t = 7 hrs, 11 hrs and 20 hrs are shown in Fig. 7. The char reactivity to O_2, H_2O, CO_2, and H_2 determines the rates for the desired product. These rates are

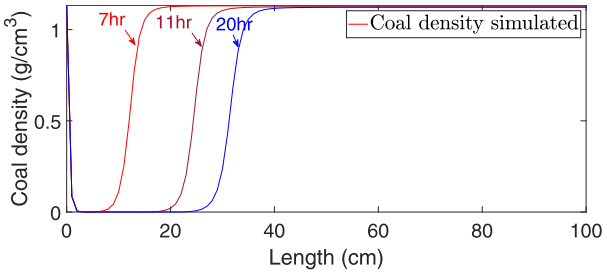

FIGURE 5. Simulated density profiles of coal.

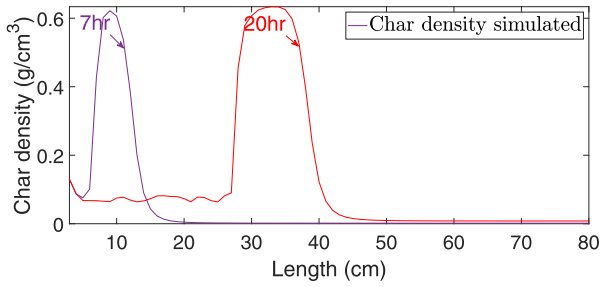

FIGURE 6. Simulated density profiles of char.

an exponential function of solid temperature that reflects the heat transfer phenomenon. The pyrolysis reaction rate is the highest at the pyrolysis front because of excess of coal. When O_2 is present, the coal decomposition process is accelerated by the oxidation reaction and CO arises as a primary syngas compound. The oxidation and the steam gasification reaction rates act as a heat source for the endothermic CO_2 gasification reaction. It is observed that the process of coal decomposition enhances above the temperature of 900K by addition of steam through the reaction $C + H_2O_{(g)} \rightarrow CO + H_2$. The increase in the H_2 concentration is due to the water-gas shift reaction. This is considerably higher for lignite coal because it consumes CO and produces more H_2, CH_4, and CO_2.

The trends of initial concentration of gases along the bed length of 1 m are shown in Fig. 8 represent the time course of values of gas components due to chemical reactions. The course concentration of CO_2 in syngas is due to production of enough heat in the oxidation zone where the combustion of carbon takes place and in the reduction zone, CO_2 reduces itself to CO. For an appropriately designed UCG reactor, production of oxygen may cause explosion in the producer, therefore O_2 and $H_2O_{(g)}$ plots show that the coal is exhausted when oxygen reduces to the zero value. The H_2 concentration is greater than CO concentration due to higher steam gasification reaction rate. Tar is produced as a by-product of the gasification process with very little concentration which can be observed at density profile of char.

The gross calorific value of the syngas in (20) is calculated on a dry basis using the sum of heating values of individual combustible constituents [40]. This calculation is based on exit concentrations of CO, H_2, CH_4, and tar only.

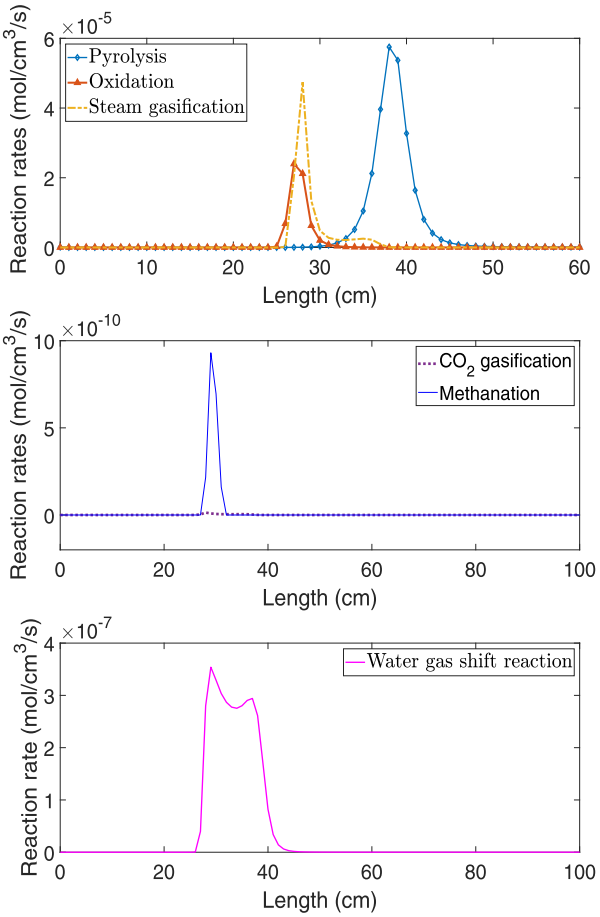

FIGURE 7. Chemical reaction rates.

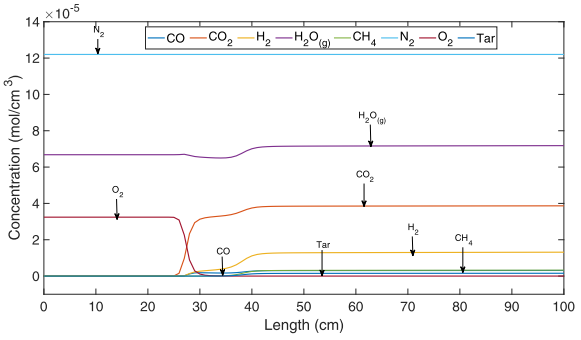

FIGURE 8. Initial concentration of gases along the length of reactor.

Mathematically,

$$HV = y_{CO}H_{CO} + y_{H_2}H_{H_2} + y_{CH_4}H_{CH_4} + y_{tar}H_{tar},$$
$$y_i = \frac{C_i}{C_T}, \tag{20}$$

where H_i is the heat of combustion of the combustible component i (kJ/m^3), y_i is the mole fraction of the gas i in the product gas on a dry basis and C_T is the sum of concentration of all gases except H_2O.

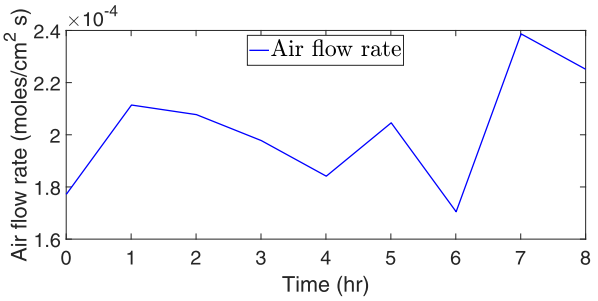

FIGURE 9. Air flow rate.

VI. MODEL COMPARISON WITH EXPERIMENTAL DATA

The GFEM based numerical model of reactor has been validated by comparing the predicted results against the field trials in block-V of Thar UCG setup. This validation requires a proper selection of input parameters and mesh. The flow rate of the inlet oxidant is taken from the experiment, shown in Fig. 9. This model validation is performed for 8 hours and records the composition of exhaust gases and the resultant heating value of syngas.

Fig. 10 represents the resulting composition of syngas for GFEM and FDM models based on the experimental data. As shown, fractions of important compounds, i.e. H_2, CH_4, and CO, vary significantly depending on a gasification process involved. This wide variation of composition determines the end use of the product gas due to its detailed spatial and temporal history by energy concentration and the chemical species. The lower concentration of CO in the product gas is due to lower temperatures. But a higher content of CH_4 can increase the overall heating value of syngas.

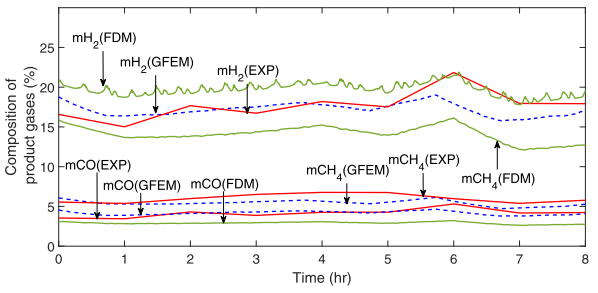

FIGURE 10. Experimental and simulated molar compositions.

There is a correlation between the flow rate of air and calorific content of syngas. The predicted HV in the GFEM model approaches the experimental HV when finer mesh is used for spatial discretization. Therefore, h = 0.3 cm, h = 0.4 cm and h = 0.5 cm were considered for the simulation of HV of syngas, with results shown in Fig. 11.

The quantitative measure of convergence is done by comparing the numerical solutions with the experiment [41], [42]. We consider the L_2 norm of residual [43]

$$\text{Error}_{(L_2)} = \left(\frac{\|u^{exp} - u^{sim}\|_{L_2}}{\|u^{exp}\|_{L_2}}\right) \times 100, \tag{21}$$

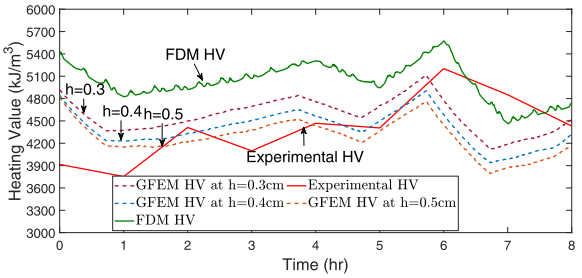

FIGURE 11. Syngas heating value.

TABLE 4. % Relative error in GFEM and FDM model parameters compared to experimental results.

Parameter	GFEM Model Error (%) h=0.3 cm	h=0.4 cm	h=0.5 cm	FDM Model Error (%)
Syngas HV	10.58	10.44	11.29	13.41
m_{CO}	28.35	31.53	34.62	133.51
m_{CH_4}	34.81	31.90	30.57	30.78
m_{H_2}	7.78	8.98	11.56	10.78

where u^{exp} is the experimental value and u^{sim} is the simulated value.

The difference between the computed results and the experimental data arises due to the approximations made in the discretization process and an iterative procedure used to solve the coupled non-linear equations of the reactor model. We have compared the experimental data with the numerical solution produced by simulation of the reactor to validate the model.

The relative errors in both models (GFEM and FDM) using the same data are reported in Table. 4. In the FDM model, we obtain one algebraic equation per grid node and the variable value appears as unknown other than node points so the error tends to be larger. The GFEM model satisfies the boundary conditions and each element is defined by continuous piece-wise polynomial functions to produce a solution in the continuous time domain. An appropriate time step size Δt is selected to maintain stability throughout the simulations because the explicit time marching scheme allows only small time steps. To reduce the error in the GFEM model, the finite element mesh is refined until the L_2 norm of the errors gets sufficiently small. According to the computed results, greater accuracy is obtained with a more refined mesh as well as with smaller time step.

A sharp change in temperature profiles was observed at the reaction front for the FDM modeling of packed bed reactor [18]. This gave rise to oscillations in the molar compositions and the HV of syngas, as seen in Fig. 10 and Fig. 11. But the integral form of the GFEM model produces stable and more accurate solution because of the positive definite stiffness matrix form of equation. This smoother behavior depicts a gradual change in the temperature distribution (Fig. 3). Although GFEM requires more programming effort, exploiting sparsity of FE matrices reduces the computer memory requirement and the computational time.

VII. CONCLUSION

A simplified one-dimensional numerical model of the packed bed reactor for the UCG process has been developed successfully. This numerical model simulates the temperature profiles in coal seam through the reactor during gasification, mass and heat transport, and the chemical reactions during coal combustion process. We have employed GFEM approach to discretize the solid phase PDEs with explicit time integration method and used implicit solvers to find solution of gas phase ODEs. The GFEM based model ensures stability of the computation of the gasification process, improves the accuracy of the computed heating value of syngas, and the composition of the combustible gas. The computational results have been compared with FDM based one-dimensional model and a good agreement has been found between the GFEM model based simulated results and experiment. The GFEM model is computationally more efficient than the FDM model for simulation of the UCG process that ensures a closer prediction of the combustion state. Lower order piece-wise basis functions are used in the GFEM model in order to simplify computations and to make a compromise between the computational effort and accuracy. In future, higher-order polynomials can be employed to explore the accuracy and complexity in the system model.

APPENDIX A
MODEL PARAMETERS

The expressions for the following mode parameters have been taken from [18], [33].

1) THERMAL CONDUCTIVITY OF SOLID

$$k = \frac{1-\phi}{\frac{1}{\lambda_s} + \frac{1}{25\lambda_g + dL_s}} + \phi d L_v \tag{A.1}$$

$$L_s = 3.16 \times 10^{-12} T_s^3$$

$$L_v = \frac{5.1 \times 10^{-12} T_s^3}{1 - 0.125\left(\frac{\phi}{1-\phi}\right)} \tag{A.2}$$

2) INTERPHASE HEAT TRANSPORT COEFFICIENT

$$h = 3C_g u_g^{0.49} T^{1.5} \left[\frac{6(1-\phi)}{d}\right]^{0.51} \times 10^{-5} \tag{A.3}$$

APPENDIX B
CHEMICAL REACTION RATES

The expressions for the following chemical reaction rates have been taken from [18], [33].

3) COAL PYROLYSIS REACTION RATE

$$r_1 = 5\frac{\rho_1}{M_1} \exp\left(\frac{-6039}{T_s}\right) \tag{B.1}$$

where ρ_1 and M_1 are density and molecular weight of coal respectively.

4) CHAR OXIDATION REACTION RATE

$$r_2 = \frac{1}{\frac{1}{r_{c_2}} + \frac{1}{k_y y_7}}$$
$$r_{c_2} = \frac{9.55 \times 10^8 \rho_2 y_7 P \exp\left(\frac{-22142}{\tilde{T}}\right) \tilde{T}^{-0.5}}{M_2}$$
$$\tilde{T} = \beta T_s + (1-\beta)\, T \tag{B.2}$$

where ρ_2 is char density, M_2 is the molecular weight of char and y_7 is the mole fraction of O_2. For simulations $\beta = 1$

5) STEAM GASIFICATION REACTION RATE

$$r_3 = \begin{cases} \dfrac{1}{\frac{1}{r_{c_3}} + \frac{1}{k_y y_4}}, & \text{if } y_4 - \left(\dfrac{y_1 y_3}{K_{E_3}}\right) > 0 \\ \dfrac{1}{\frac{1}{R_{c_3}} - \frac{1}{k_y y_1}}, & \text{if } y_4 - \left(\dfrac{y_1 y_3}{K_{E_3}}\right) < 0 \end{cases}$$
$$r_{c_3} = \frac{{r_{c_3}}^+}{y_4}\left(y_4 - \frac{y_1 y_3}{K_{E_3}}\right)$$
$${r_{c_3}}^+ = \frac{\rho_2 y_4^2 P^2 \exp\left(5.052 - \frac{12908}{\tilde{T}}\right)}{M_2\left[y_4 P + \exp\left(-22.216 + \frac{24880}{\tilde{T}}\right)\right]^2} \tag{B.3}$$

where y_1,y_3 and y_4 are molar fractions of CO, H_2 and H_2O respectively, and K_{E_3} is equilibrium constant for steam gasification reaction.

6) CO_2 GASIFICATION REACTION RATE

$$r_4 = \begin{cases} \dfrac{1}{\frac{1}{r_{c_4}} + \frac{1}{k_y y_2}}, & \text{if } y_2 - \left(\dfrac{y_1^2}{K_{E_4}}\right) < 0 \\ \dfrac{1}{\frac{1}{r_{c_4}} - \frac{2}{k_y y_1}}, & \text{if } y_2 - \left(\dfrac{y_1^2}{K_{E_4}}\right) > 0 \end{cases}$$
$$r_{c_4} = \frac{{r_{c_4}}^+}{y_2}\left(y_2 - \frac{y_1^2}{K_{E_4}}\right)$$
$${r_{c_4}}^+ = \frac{1.15 \times 10^4 \rho_2 y_2 P \exp\left(\frac{-23956}{\tilde{T}}\right)}{M_2 D}$$
$$D = 1 + 0.014 y_1 P \exp\left(\frac{7549}{\tilde{T}}\right) + 0.21 y_2 P \exp\left(\frac{3171}{\tilde{T}}\right) \tag{B.4}$$

where y_2 is the mole fraction of CO_2, and K_{E_4} is equilibrium constant for CO_2 gasification reaction.

7) METHANATION REACTION RATE

$$r_5 = \begin{cases} \dfrac{1}{\frac{1}{r_{c_5}} + \frac{2}{k_y y_3}}, & \text{if } y_3^2 - \left(\dfrac{y_5}{K_{E_5}}\right) > 0 \\ \dfrac{1}{\frac{1}{r_{c_5}} - \frac{1}{k_y y_5}}, & \text{if } y_3^2 - \left(\dfrac{y_5}{K_{E_5}}\right) < 0 \end{cases}$$
$$r_{c_5} = \frac{{r_{c_5}}^+}{y_3^2}\left(y_3^2 - \frac{y_5}{K_{E_5}}\right)$$
$${r_{c_5}}^+ = \frac{\rho_2 y_3^2 P^2 \exp\left(2.803 - \frac{13673}{\tilde{T}}\right)}{M_2\left[1 + y_3 P \exp\left(-10.452 + \frac{11698}{\tilde{T}}\right)\right]} \tag{B.5}$$

where y_5 is mole fraction of CH_4, and K_{E_5} is equilibrium constant for methanation reaction.

8) WATER GAS SHIFT REACTION RATE

$$r_6 = \begin{cases} \dfrac{1}{\frac{1}{r_{c_6}} + \frac{2}{k_y y_1}}, & \text{if } C_1 C_4 - \left(\dfrac{C_2 C_3}{K_{E_6}}\right) > 0 \\ \dfrac{1}{\frac{1}{R_{c_6}} - \frac{1}{k_y y_2}}, & \text{if } C_1 C_4 - \left(\dfrac{C_2 C_3}{K_{E_6}}\right) < 0 \end{cases}$$
$$r_{c_6} = \frac{{R_{c_6}}^+}{C_1 C_4}\left(C_1 C_4 - \frac{C_2 C_3}{K_{E_6}}\right)$$
$${r_{c_6}}^+ = 3 \times 10^7 \phi C_1 C_4 \exp\left(\frac{-7250}{\tilde{T}}\right) \tag{B.6}$$

where C_1, C_2, C_3 and C_4 are concentrations of CO, CO_2, H_2 and H_2O respectively, and K_{E_6} is equilibrium constant for water gas shift reaction.

REFERENCES

[1] S. J. Friedmann, R. Upadhye, and F.-M. Kong, "Prospects for underground coal gasification in carbon-constrained world," *Energy Procedia*, vol. 1, no. 1, pp. 4551–4557, Feb. 2009.
[2] D. A. Bell, B. F. Towler, and M. Fan, "Underground coal gasification," in *Coal Gasification and its Applications*. Boston, MA, USA: William Andrew Publishing, 2011, Ch. 3, pp. 35–71.
[3] M. Blinderman and R. Jones, "Underground coal gasification and power generation," Coal New Horiz., Gasification Technol. Conferens, San Francisco, CA, USA, Tech. Rep., 2002.
[4] A. W. Bhutto, A. A. Bazmi, and G. Zahedi, "Underground coal gasification: From fundamentals to applications," *Prog. Energy Combustion Sci.*, vol. 39, no. 1, pp. 189–214, Feb. 2013.
[5] *World Energy Resources: 2013 Survey*, WEC, London, U.K., 2013.
[6] M. S. Malkani, A. M. K. MH, F. Buzdar, and M. Zahid, "Coal Resources of Pakistan: New coalfields," *Lasbela Univ. J. Sci. Technol.*, vol. 5, pp. 7–22, Jul. 2016.
[7] A. Y. Malik, M. I. Ali, A. Jamal, U. Farooq, N. Khatoon, W. H. Orem, E. P. Barnhart, J. R. SanFilipo, H. He, and Z. Huang, "Coal biomethanation potential of various ranks from pakistan: A possible alternative energy source," *J. Cleaner Prod.*, vol. 255, May 2020, Art. no. 120177.
[8] M. Khan, J. Mmbaga, A. Shirazi, Q. Liu, and R. Gupta, "Modelling underground coal gasification—A review," *Energies*, vol. 8, no. 11, pp. 12603–12668, 2015.
[9] S. B. Javed, A. A. Uppal, A. I. Bhatti, and R. Samar, "Prediction and parametric analysis of cavity growth for the underground coal gasification project thar," *Energy*, vol. 172, pp. 1277–1290, Apr. 2019.
[10] V. V. Ranade, S. M. Mahajani, and G. A. Samdani, *Computational Modeling of Underground Coal Gasification*. Boca Raton, FL, USA: CRC Press, 2019.
[11] M. Seifi, "Simulation and modeling of underground coal gasification using porous medium approach," Ph.D. dissertation, Dept. Chem. Petroleum Eng., Univ. Calgary, Calgary, AB, Canada, 2014.
[12] R. D. Gunn and D. L. Whitman, "An in-situ coal gasification model (forward mode) for feasibility studies and design," Laramie Energy Res. Center, Laramie, WY, USA, Tech. Rep. LERC/RJ-76/2, 1976.
[13] C. Thorsness and R. Rosza, "Lawrence Livermore Laboratory *in-situ* coal gasification program: Model calculations and laboratory experiments," New Orleans, LA, USA, Tech. Rep., 1976.
[14] C. Thorsness, E. Grens, and A. Sherwood, "One-dimensional model for *in situ* coal gasification," Lawrence Livermore Lab., California Univ., Livermore, CA, USA, Tech. Rep. UCRL-52523, 1978.

[15] A. Winslow, "Numerical model of coal gasification in a packed bed," *Symp. (Int.) Combustion*, vol. 16, no. 1, pp. 503–513, 1977.
[16] E. A. A. Abdel-Hadi and T. R. Hsu, "Computer modeling of fixed bed underground coal gasification using the permeation method," *J. Energy Resour. Technol.*, vol. 109, no. 1, pp. 11–20, Mar. 1987.
[17] A. Khadse, M. Qayyumi, and S. Mahajani, "Reactor model for the underground coal gasification (UCG) channel," *Int. J. Chem. React. Eng.*, vol. 4, no. 1, pp. 2–4 and 12–20, 2006.
[18] A. A. Uppal, A. I. Bhatti, E. Aamir, R. Samar, and S. A. Khan, "Control oriented modeling and optimization of one dimensional packed bed model of underground coal gasification," *J. Process Control*, vol. 24, no. 1, pp. 269–277, Jan. 2014.
[19] A. A. Uppal, Y. M. Alsmadi, V. I. Utkin, A. I. Bhatti, and S. A. Khan, "Sliding mode control of underground coal gasification energy conversion process," *IEEE Trans. Control Syst. Technol.*, vol. 26, no. 2, pp. 587–598, Mar. 2018.
[20] J. Douglas and T. Dupont, "Galerkin methods for parabolic equations," *SIAM J. Numer. Anal.*, vol. 7, no. 4, pp. 575–626, 1970.
[21] G. A. Baker, J. H. Bramble, and V. Thomée, "Single step Galerkin approximations for parabolic problems," *Math. Comput.*, vol. 31, no. 140, pp. 818–847, 1977.
[22] H. A. Jakobsen, H. Lindborg, and V. Handeland, "A numerical study of the interactions between viscous flow, transport and kinetics in fixed bed reactors," *Comput. Chem. Eng.*, vol. 26, no. 3, pp. 333–357, Mar. 2002.
[23] H. A. Jakobsen, "Numerical convection algorithms and their role in Eulerian CFD reactor simulations," *Int. J. Chem. React. Eng.*, vol. 1, no. 1, pp. 3–5, Oct. 2002.
[24] O. P. Yadav and R. Jiwari, "A finite element approach for analysis and computational modelling of coupled reaction diffusion models," *Numer. Methods Partial Differ. Equ.*, vol. 35, no. 2, pp. 830–850, Mar. 2019.
[25] F. Dubeau, A. Ouansafi, and A. Sakat, "Galerkin methods for nonlinear ordinary differential equation with impulses," *Numer. Algorithms*, vol. 33, nos. 1–4, pp. 215–225, 2003.
[26] O. P. Yadav and R. Jiwari, "Finite element analysis and approximation of Burgers'-Fisher equation," *Numer. Methods Partial Differ. Equ.*, vol. 33, no. 5, pp. 1652–1677, 2017.
[27] V. Thomée, *Galerkin finite Element Methods for Parabolic Problems*, vol. 1054. Berlin, Germany: Springer, 1984.
[28] U. M. Ascher and L. R. Petzold, *Computer Methods for Ordinary Differential Equations and Differential-Algebraic Equations*, vol. 61. Philadelphia, PA, USA: SIAM, 1997.
[29] J. Wang and X. Ye, "A weak Galerkin mixed finite element method for second order elliptic problems," *Math. Comput.*, vol. 83, no. 289, pp. 2101–2126, May 2014.
[30] H. A. Jakobsen, *Chemical Reactor Modeling*. Berlin, Germany: Springer, 2014.
[31] S. C. Chapra and R. P. Canale, *Numerical Methods for Engineers*. Boston, MA, USA: McGraw-Hill, 2010.
[32] T. Chang, J. van Hulzen, and P. S. Wang, "Code generation and optimization for finite element analysis," in *Proc. Int. Symp. Symbolic Algebr. Manipulation*. Berlin, Germany: Springer, 1984, pp. 237–247.
[33] A. A. Uppal, "Modeling and control of underground coal gasification," Ph.D. dissertation, Dept. Elect. Eng., COMSATS Inst. Inf. Technol., Islamabad, Pakistan, 2016.
[34] A. A. Uppal, A. I. Bhatti, E. Aamir, R. Samar, and S. A. Khan, "Optimization and control of one dimensional packed bed model of underground coal gasification," *J. Process Control*, vol. 35, pp. 11–20, Nov. 2015.
[35] S. Zhou, F. Gao, B. Li, and Z. Sun, "Weak Galerkin finite element method with second-order accuracy in time for parabolic problems," *Appl. Math. Lett.*, vol. 90, pp. 118–123, Apr. 2019.
[36] L. Yang and S. Liu, "Numerical simulation on heat and mass transfer in the process of underground coal gasification," *Numer. Heat Transf., A, Appl.*, vol. 44, no. 5, pp. 537–557, Oct. 2003.
[37] M. E. Hosea and L. F. Shampine, "Analysis and implementation of TR-BDF2," *Appl. Numer. Math.*, vol. 20, nos. 1–2, pp. 21–37, Feb. 1996.
[38] Y. Lu-feng, "TR-BDF2 method for solving the ordinary differential equations," *J. Yunnan Univ. Nationalities (Natural Sci. Ed.)*, vol. 3, p. 8, Mar. 2013.
[39] S. Adjerid and J. E. Flaherty, "A moving-mesh finite element method with local refinement for parabolic partial differential equations," *Comput. Methods Appl. Mech. Eng.*, vol. 55, nos. 1–2, pp. 3–26, Apr. 1986.
[40] J. H. Harker and J. R. Backhurst, *Fuel and Energy*. New York, NY, USA: Academic, 1981, p. 373.
[41] I. Babuska and B. Szabo, "On the rates of convergence of the finite element method," *Int. J. Numer. Methods Eng.*, vol. 18, no. 3, pp. 323–341, Mar. 1982.
[42] G. J. Fix and J. P. Roof, "Least squares finite-element solution of a fractional order two-point boundary value problem," *Comput. Math. Appl.*, vol. 48, nos. 7–8, pp. 1017–1033, Oct. 2004.
[43] K. S. Surana, A. D. Joy, and J. N. Reddy, "Error estimations, error computations, and convergence rates in FEM for BVPs," *Appl. Math.*, vol. 7, no. 12, pp. 1359–1407, 2016.

QUDSIYA IRUM received the B.S. degree from the University College of Engineering Mirpur, Pakistan, in 2010, and the M.S. degree from COMSATS University Islamabad (CUI), Pakistan, in 2013, where she is currently pursuing the Ph.D. degree. She has been working as a Lecturer with CUI since 2013. Her research interests include modeling, numerical solution, smart grid systems, renewable/green energy, and finite element method.

SHAHID A. KHAN received the B.S. degree in electrical engineering from the University of Engineering and Technology, Lahore, Pakistan, and the M.S. and Ph.D. degrees in radio communications from the Universality of Portsmouth, U.K. In 2003, he joined COMSATS University Islamabad (CUI) as an Assistant Professor and elevated to a Professor within few years. He worked as the HOD, the Chairman, and the Dean of the Faculty of Engineering. He is currently the Founder of various engineering programs in different campuses of CIIT. He has established many teaching and research labs by securing funding of about ten million USD. He has authored over 80 research articles published in international journals and conferences. On the basis of his meritorious services, he has been honored with multiple awards and memberships in the field of engineering education.

ALI ARSHAD UPPAL (Member, IEEE) received the B.E. and M.S. degrees in electrical and computer engineering from the University of Engineering and Technology Taxila, Taxila, Pakistan, in 2006 and 2012, respectively, and the Ph.D. degree in electrical engineering from COMSATS University Islamabad (CUI), Pakistan, in 2016. He is currently working as a Postdoctoral Researcher on the UPWIND Project with the Department of Electrical and Computer Engineering, University of Porto. He is also an Assistant Professor with COMSATS University Islamabad. So far, he has authored/coauthored 14 journal publications in peer reviewed impact factor journals. His research interests include nonlinear control, sliding mode control, process control, numerical optimal control, and control of infinite dimensional systems.

LILIA KRIVODONOVA received the B.S. and M.S. degrees from St. Petersburg State University, Russia, and the Ph.D. degree from the Rensselaer Polytechnic Institute, USA. She is currently an Associate Professor and an Associate Chair of the Graduate Studies, Department of Applied Mathematics, University of Waterloo, Canada. Her research interests include discontinuous Galerkin methods, error estimation and adaptive methods, finite element methods, and high-order numerical methods for hyperbolic partial differential equations.